CONF-820604--9

# STEADY-STATE FILM-BOILING DATA IN ROD-BUNDLE GEOMETRY AND NON-EQUILIBRIUM CORRELATION ASSESSMENT*

G. L. Yoder
D. G. Morris
C. B. Mullins
L. J. Ott
D. A. Reed

Oak Ridge National Laboratory
Oak Ridge, Tennessee 37830

ABSTRACT

A series of 22 steady-state, rod bundle, dispersed flow film boiling experiments has been performed at the Oak Ridge National Laboratory (ORNL) in the Thermal-Hydraulic Test Facility (THTF), a pressurized-water loop containing 64 full-length electrically heated rods. Test parameters in the upflow experiments cover a wide range of conditions typical of those which might be encountered during a nuclear reactor loss-of-coolant accident.

Local equilibrium fluid conditions were calculated using mass and energy conservation considerations. Experimentally determined heat transfer coefficients were compared to several available film boiling heat transfer correlations: Dougall-Rohsenow, Groeneveld 5.7, Groeneveld-Delorme, Chen, Jones-Zuber, and Yoder-Rohsenow.

The Groeneveld 5.7 correlation tended to predict the data better than any other correlation tested. The Dougall-Rohsenow correlation tends to overpredict the data while the Yoder-Rohsenow correlation predicted the data better than the other non-equilibrium correlations examined. However, all of the non-equilibrium correlations generally underpredict the heat transfer.

CONF-820604--9

DE82 017479

MASTER

*Research sponsored by Division of Reactor Safety Research, U.S. Nuclear Regulatory Commission under Interagency Agreements DOE 40-551-75 and 40-552-75 with the U.S. Department of Energy under contract W-7405-eng-26 with the Union Carbide Corporation.

## INTRODUCTION

Film boiling is a two-phase heat transfer regime which occurs when heated surface temperatures are high enough to prevent intimate liquid surface contact. Film boiling is present in steam generators, some refrigeration equipment, and may occur during a nuclear reactor loss-of-coolant accident (LOCA). It is characterized by surface temperatures which may be high enough to cause material damage. It is therefore important to distinguish this regime both theoretically and experimentally.

Previous experimental efforts resulted in large amounts of tube and annuli film boiling data [1-3]. However, the amount of rod bundle data available remains limited [4]. Results of this experimental investigation should improve the rod bundle data base and prove useful in film boiling correlation development and assessment. A complete listing of all film boiling data acquired in the steady-state tests can be found in Ref. 5.

The methods of predicting film boiling heat transfer generally follow one of three paths. One method is to simply correlate film boiling data. An example of this method is the series of Groeneveld 5.7 correlations [6], which were developed from tube and annuli data. The Groeneveld 5.7 correlation is evaluated in this paper. A good review of such correlations is given in Ref. 7. The primary advantage of this approach is the simplicity of the solutions obtained. However, extrapolation of the correlation beyond the data base must be done with caution.

The second method integrates the energy, momentum, and mass transport equations along the flow path. A two- or three-step heat transfer process is normally assumed with heat transfer interactions between the wall, the vapor, and the liquid present in the flow. By separating the flow into separate liquid and vapor components, thermal non-equilibrium can be included in the analysis. Several investigators have used this approach for different fluids with varying degrees of success [8-10].

The third method attempts to combine the above two approaches by explicitly accounting for non-equilibrium within the flow. Typically this approach assumes that film boiling heat transfer can be characterized by a single-phase vapor heat transfer coefficient. Both Chen [11] and Groeneveld [12] have correlated non-equilibrium within the flow (and therefore actual quality) using film boiling data and assuming the heat transfer is primarily through the vapor. Jones [13] and Yoder [14] have each used the governing transport equations to develop methods of predicting non-equilibrium within the flow. These four non-equilibrium correlations are all evaluated in this paper.

The Dougall-Rohsenow correlation [15], which is used in many reactor codes, does not fit neatly into any of the above methods. It was developed from the single-phase Dittus-Boelter equation assuming that the vapor velocity could be evaluated from the local equilibrium quality. Thus, analysis using the Dougall-Rohsenow correlation does not include non-equilibrium effects.

## FACILITY DESCRIPTION AND EXPERIMENTAL PROCEDURE

A series of 22 steady-state film boiling experiments was performed at the Oak Ridge National Laboratory in the Thermal-Hydraulic Test Facility, a high-temperature, pressurized-water loop containing an 8 x 8 electrically heated rod bundle. The 3.66-m (12-ft) rods are arranged in a configuration typical of later generation pressurized-water reactors with 17 x 17 fuel assemblies. A schematic of the THTF loop is shown in Fig. 1. Flow measurement sites are positioned at each end of the test section containing the

rod bundle. The bundle is heavily instrumented with thermocouples positioned at various axial levels as shown in Fig. 2. Spacer grids are located at 0.6-m (2-ft) intervals along the heated length. Four unheated rods are located at positions corresponding to control rod locations within an actual fuel assembly (Fig. 3). Both axial and radial power profiles are flat. Rods have a 0.95-cm (0.374-in.) diam with pitch of 1.27 cm (0.501 in.) and the bundle hydraulic diameter is 1.06 cm (0.4178 in.). During some of the tests (~23%), rod 32, normally a heated rod, was unheated.

During steady-state operation of the THTF, fluid flows from the pump (Fig. 2) through two flow control valves and several measurement spool pieces before it enters the test section. Fluid is heated as it flows past the rods in the test section and leaves the upper plenum passing through three outlet spool pieces and several heat exchangers before returning to the pump.

Each steady-state test was performed by initially establishing inlet flow to the test section and adjusting the loop to provide the desired inlet fluid temperature and pressure. Bundle power was then increased until the dryout point was at the desired location within the bundle. The steady-state operating point was assumed to have been reached when operating pressure and rod surface temperature stabilized. Instruments were scanned for 20 s during each experiment. Data were averaged over this 20-s interval to arrive at local rod surface conditions.

## DATA AND CORRELATIONS

All 22 steady-state experiments were upflow experiments designed to facilitate calculation of local bundle equilibrium fluid conditions. In all tests inlet fluid was subcooled to insure accurate flow measurement. Local equilibrium fluid conditions could then be calculated using simple mass and energy conservation considerations. Test parameters covered a wide range of fluid and surface conditions typical of a postulated nuclear reactor loss-of-coolant accident:

| | |
|---|---|
| Mass flux, kg/m²/s (lb$_m$/ft²/h) | 814-225 (6-1.7 x $10^6$) |
| Heat flux, kW/m²/s (Btu/ft²/h) | 945-315 (3-1 x $10^6$) |
| Equilibrium quality, % | 130-40 |
| Pressure, MPa (psi) | 13-4.4 (1900-635) |

The steady-state data have been compared to several film boiling correlations including:

1. Dougall-Rohsenow [15]
2. Groeneveld 5.7 [6]
3. Chen [11]
4. Groeneveld-Delorme [12]
5. Jones-Zuber [13]
6. Yoder-Rohsenow [14]

As stated previously, the Dougall-Rohsenow correlation is basically a single-phase Dittus-Boelter heat transfer coefficient with the velocity evaluated at the local equilibrium vapor velocity

$$h = 0.023 \frac{k_g}{D} Pr_g^{0.4} \left\{ Re_g \left[ X + \frac{\rho_g}{\rho_f} (1 - X) \right] \right\}^{0.8} .$$

The Groeneveld 5.7 correlation is an equation developed from film boiling data in annuli

$$h = \frac{0.052 \frac{k_g}{D} Pr_w^{1.26} \left\{ Re_g \left[ X + \frac{\rho_g}{\rho_f} (1 - X) \right] \right\}^{0.688}}{\left[ 1.0 - 0.1 (1 - X)^{0.4} \left( \left( \frac{\rho_f}{\rho_g} \right) - 1 \right)^{0.4} \right]^{1.26}} .$$

The non-equilibrium correlation developed by Chen can be divided into two separate parts. The first is a correlated relationship which allows calculation of actual quality (including non-equilibrium) from *local equilibrium fluid conditions*.

$$\frac{X_A}{X} = 1.0 - B\left[\frac{T_v - T_s}{T_w - T_v}\right],$$

where

$$B = 0.26/[1.15 - (P/P_c)^{0.45}]$$

and knowing

$$\frac{X_A}{X} = i_{fg}/(i_v - i_f) .$$

The second is a vapor heat transfer coefficient based on actual quality and actual vapor temperature

$$h = G\, X_A\, C_{p,f}\, Pr_f^{-2/3}\, f/2 ,$$

where

$$f = 0.037\left\{\frac{GD}{\mu_v}\left[\frac{\rho_v}{\rho_f}(1 - X_A) + X_A\right]\right\}^{-0.17} .$$

The Groeneveld-Delorme correlation is similar to Chen's in that it is a correlation which predicts actual vapor enthalpy (and therefore quality) from local equilibrium conditions.

$$\frac{i_v - i}{i_{fg}} = \exp(-\tan\psi)\exp[1-(3\,a_{hom})^{-4}] .$$

$\psi$ and $a_{hom}$ are *functions of equilibrium fluid conditions*. It also utilizes the Hadaller steam heat transfer coefficient using actual vapor quality and temperature

$$h = 0.0083\frac{k_f}{D}\left\{\frac{GD}{\mu_f}\left[X_A + \frac{\rho_v}{\rho_f}(1 - X_A)\right]\right\}^{0.877} Pr_f^{0.61} .$$

The Jones-Zuber equation was developed from the governing transport equations and treats the vapor-to-droplet heat transfer as a relaxation process. The relationship between actual quality and equilibrium quality is a differential equation and requires stepwise integration along the flow path beginning at the dryout point (the point where liquid can no longer come in intimate contact with the heated surface). However, this integration is much simpler than those needed when integrating the entire set of transport equations

$$\frac{d(X - X_A)}{dX} + N_{SR}(X - X_A) = 1 .$$

$N_{SR}$ is a correlated parameter based on actual local fluid conditions and system pressure. Once actual fluid conditions are known (including non-equilibrium) the Dittus-Boelter single-phase vapor heat transfer coefficient is used to calculate surface temperatures given surface heat fluxes

$$h = 0.023\frac{k_v}{D}\left(\frac{GDX_A}{\mu_v a_A}\right)^{0.8} Pr_v^{0.4} .$$

The Yoder-Rohsenow equations are similar to the Jones-Zuber solution in that they use the governing transport equations to develop a method for calculating actual quality given equilibrium fluid conditions. However, no correlated parameters are used in their approach. The result of their analysis is also a differential equation which requires step-wise integration

$$K \frac{X_A^{2/4}\, X}{(1 - X_A)^{7/12}} \frac{dX_A}{dX} = (X - X_A) .$$

The equation for the constant K is a function of saturated fluid and dryout conditions alone. Integration of this equation therefore results in a series of curves relating actual quality to equilibrium quality as a function of the parameter K and burnout quality. Similar to the methods described above, actual quality and actual vapor properties are used to evaluate a single-phase vapor heat transfer coefficient (Heineman) to calculate heated wall temperatures given surface heat fluxes. For the THTF data, the Heineman equation [16] was evaluated at L/D = 29, the point midway between grids.

$$h = 0.0137 \frac{k_f}{D} \left( \frac{GDX_A}{\mu_f \alpha_A} \right)^{0.84} Pr_f^{1/3} .$$

RESULTS

Data presented in this paper are only from locations midway between the spacer grids in order to eliminate the effects of the grid on the local heat transfer. The steady state tests were all dispersed flow tests, and film boiling was assumed to exist only when the wall superheat was 222°C (400°F) or higher. Results of all of the steady-state tests are presented as plots of experimental values on the ordinate versus predicted values on the abscissa. The quantity plotted depends on the correlation being evaluated.

The Dougall-Rohsenow comparison is shown plotted in Fig. 4. The experimental heat transfer coefficient is defined as $h_{exp} = Q''/T_w - T_s$. Any point above and to the left of the diagonal line indicates that the correlation underpredicts the data, while any point below and to the right of the diagonal line indicates that the correlation overpredicts the heat transfer. Each vertical string is data taken at one axial location. Vertical scatter indicates a variation in the heat transfer coefficient at one axial location. Since measurement error in the experimental heat transfer coefficient is estimated to be ~10% (1 σ), the vertical scatter seems to be dne to radial variations in the fluid conditions.

In general, the Dougall-Rohsenow correlation tends to overpredict the data, sometimes as much as 250%. The correlation does not include non-equilibrium effects. These effects would be expected to be present under most film boiling conditions. Non-equilibrium in the flow would tend to decrease the experimental heat transfer coefficient over that which would be expected under equilibrium conditions by reducing the local vapor Reynolds number and increasing the local vapor temperature. Thus, the Dougall-Rohsenow correlation would tend to overpredict the data as it does in Fig. 4.

The Groeneveld 5.7 comparison is presented in Fig. 5. The experimental heat transfer coefficient is defined as $h_{exp} = Q''/T_w - T_s$. Again, each data string represents one axial level within the bundle. The slight slant in each string reflects the effect

of a surface temperature variation on the wall Prandtl number evaluated in the Groeneveld 5.7 correlation. This correlation generally predicts heat transfer coefficients better than any of the other correlations presented in this paper.

A comparison of data with the Chen correlation is presented in Fig. 6. As input, the Chen correlation requires the surface temperature and calculates the surface heat flux. Experimental heat flux is therefore plotted on the ordinate while predicted heat flux is plotted on the abscissa. In general, the Chen correlation tends to underpredict the heat transfer in these tests. The form of the Chen correlation is such that non-equilibrium is predicted to exist even at the dryout point where equilibrium conditions would be expected. Thus heat fluxes predicted by the Chen correlation near dryout would tend to be lower than those actually experienced.

Figure 7 is a plot of the Groeneveld-Delorme comparison. This correlation requires surface heat flux as input and calculates surface temperature. Experimental wall superheats are plotted on the ordinate with correlation predicted superheats plotted on the abscissa. In this type of plot, any point lying above and to the left of the diagonal line indicates an overprediction of the heat transfer by the correlation while any point lying below and to the right of the diagonal line indicates an underprediction of the heat transfer by the correlation. Figure 7 shows that the Groeneveld-Delorme equation tends to underpredict the heat transfer. Although difficult to detect from the figure, this correlation tends to do better as the distance from dryout increases. Similar to the Chen correlation, the Groeneveld-Delorme correlation predicts non-equilibrium even at dryout, causing the correlation to underpredict the heat transfer.

The Jones-Zuber comparison is plotted in Fig. 8. Again, wall superheats are plotted due to the form of the correlation. The Jones-Zuber correlation tends to overpredict the heat transfer near dryout, and underpredict as distance from dryout increases. The form of the correlation dictates that equilibrium exists at dryout. As distance from dryout increases, the non-equilibrium also increases.

The Yoder-Rohsenow comparison is presented in Fig. 9. It also tends to underpredict the heat transfer, however it predicts best of the non-equilibirum correlations examined. As in the Jones-Zuber correlation, equilibrium conditions are predicted at dryout with non-equilibrium increasing as distance from dryout increases. Unlike the Chen and Groeneveld-Delorme correlations, this scheme predicts best near dryout. The underprediction of heat transfer at distances far from dryout could indicate an overprediction of the non-equilibrium present.

In general, with the possible exception of the Jones-Zuber correlation where the prediction is scattered, all of the non-equilibrium correlations tend to underpredict the heat transfer for these 22 steady-state rod bundle tests. All of these methods were either developed from tube data or were compared to tube data when first formulated. One would expect that the bundle geometry and the presence of spacers within the bundle would tend to increase the heat transfer and perhaps decrease the non-equilibrium over that which would be expected in tube experiments. This could explain the discrepancy between the non-equilibrium correlations and the bundle data. The Groeneveld 5.7 correlation, on the other hand, was developed from annuli data. It tends to predict the bundle data better than any of the other correlations tested.

Two general reasons can be identified which would cause the non-equilibrium correlations to underpredict the bundle heat transfer. If the heat transfer coefficients used in these methods were too low, the surface temperatures predicted would be too

high. (In the case of the Chen correlation, predicted heat fluxes would be too low.) Rod bundles generally have slightly higher heat transfer coefficients than do tubes of similar hydraulic diameters. With the rod pitch-to-diameter ratio in the THTF bundle, this effect is estimated to be between 5 and 10% [17]. This increase is not enough to explain the discrepancy between the THTF data and the non-equilibrium correlations' predictions. The second factor which affects the non-equilibrium correlations is the degree of non-equilibrium present in the flow. If the degree of non-equilibrium predicted is higher than that which actually exists, heat transfer predictions would tend to be low. Unfortunately, no instrumentation is available in the THTF to measure vapor superheat and therefore, non-equilibrium in the flow. Therefore, it is impossible to experimentally separate the effect of non-equilibrium and heat transfer coefficient. Methods have been developed [18] to measure vapor superheat in tube geometry. This should allow better characterization of the non-equilibrium and therefore the heat transfer in future tube correlations.

## CONCLUSIONS

Steady-state, rod bundle, film boiling data have been obtained over a wide range of flow and surface conditions. These data should prove useful in both correlation development and assessment, and should provide insight into rod bundle heat transfer characteristics.

Two conventional film boiling heat transfer coefficients were compared with the steady-state data. The Dougall-Rohsenow equation tended to overpredict the data, sometimes by as much as 250%. On the other hand, the Groeneveld 5.7 correlation which was developed from annuli data predicted the bundle data better than any other correlation examined. Four non-equilibrium correlations were also evaluated. In general, all of the non-equilibrium equations tended to underpredict the heat transfer. Both the Chen and the Groeneveld-Delorme equations predict heat transfer better as distance from dryout increases. The Jones-Zuber method underpredicts in some instances and overpredicts in others, while the Yoder-Rohsenow method, which predicts the THTF data better than the other non-equilibrium correlations examined, predicts heat near dryout.

A closer study of rod bundle heat transfer is needed to characterize the differences in rod and tube geometry.

## NOTATION

| | |
|---|---|
| $C_p$ | Specific heat at constant pressure |
| D | Hydraulic diameter [4 x flow area/wetted perimeter] |
| f | Friction factor |
| G | Bundle mass flux |
| h | Heat transfer coefficient |
| $i_{fg}$ | Heat of vaporization |
| i | Enthalpy |
| k | Thermal conductivity |
| L | Axial distance from the closest upstream grid |
| P | Pressure |

| | |
|---|---|
| Pr | Prandtl number ($C_p\mu/k$) |
| Q'' | Surface heat flux |
| $Re_g$ | Reynolds number ($DG/\mu_g$) |
| T | Temperature |
| X | Equilibrium quality |
| $X_A$ | Actual quality |
| $\alpha$ | Void fraction |
| $\rho$ | Density |
| $\mu$ | Viscosity |

SUBSCRIPTS

| | |
|---|---|
| A | Actual fluid conditions |
| c | Critical |
| exp | Experimental |
| f | Film |
| g | Saturated vapor |
| hom | Homogeneous fluid conditions |
| f | Saturated liquid |
| v | Actual vapor |
| w | Wall |

REFERENCES


1 Bennet, A. W., Hewitt, G. F., Kearsey, H. A., and Keeys, R. F. K., "Heat Transfer to Steam-Water Mixtures in Uniformly Heated Tubes in Which the Critical Heat Flux has been Exceeded," AERE-R-5373, October 1967.

2 Janssen, E. and Kervinen, J. A., "Film Boiling and Rewetting," NEDO-20975, 1975.

3 Polomik, E. E., Levy, S., and Sawochka, S. G., "Film Boiling of Steam-Water Mixtures in Annular Flow at 800, 1100, and 1400 psi," ASME paper 62-WA-136, presented at the Winter Annual Meeting, New York, NY, November 25-30, 1962.

4 Turner, D., "Blowdown Heat Transfer Program Film Boiling Heat Transfer Coefficients" (CE/Columbia Tests), CENPD-152 Revision 1, October 1975.

5 Yoder, G. L., Morris, D. G., Mullins, C. B., Ott, L. J., and Reed, D. A., "Dispersed Flow Film Boiling in Rod Bundle Geometry - Steady State Heat Transfer Data and Correlation Comparisons," ORNL/5822, to be published.

6 Groeneveld, D. C., "Post-Dryout Heat Transfer at Reactor Generating Conditions," AECL-4513, June 1973.

7 Groeneveld, D. C. and Gardiner, S. R. M., "Post-CHF Heat Transfer Under Forced Convective Conditions," AECL-5883.

8 Foralund, R. P., "Thermal Non-Equilibrium in Dispersed Flow Film Boiling in a Vertical Tube," Ph.D. Thesis, Massachusetts Institute of Technology, December 1966.

9 Hynek, S. J., "Forced Convection Dispersed Flow Film Boiling," Ph.D. Thesis, Massachusetts Institute of Technology, 1969.

10 Koizumi, Y., Ueda, T., and Tanaka, H., "Post Dryout Heat Transfer to R-113 Upward Flow in a Vertical Tube," *Int. J. of Heat and Mass Transfer*, Vol. 22, pp. 669-78.

11 Chon, J. C., Ozkaynak, F. T., and Sundaram, R. K., "Vapor Heat Transfer in Post-CHF Region Including the Effect of Thermodynamic Non-Equilibrium," *Nuclear Engineering and Design*, Vol. 51, No. 2, 1978, pp. 143-155.

12 Groeneveld, D. C. and Delorme, G. G. J., "Prediction of Thermal Non-Equilibrium in the Post-Dryout Regime," *Nuclear Engineering and Design*, Vol. 36, No. 1, pp. 17-26.

13 Jones, O. C., Jr. and Zuber, N., "Post-CHF Heat Transfer: A Non-Equilibrium Relaxation Model," ASME 77-HT-79, presented at the AIChE-ASME Heat Transfer Conference, Salt Lake City, Utah, August 15-17, 1977.

14 Yoder, G. L. and Rohsenow, W. M., "Dispersed Flow Film Boiling," MIT Heat Transfer Laboratory Report No. 85694-103, March 1980.

15 Dougall, R. L. and Rohsenow, W. M., "Film Boiling on the Inside of Vertical Tubes with Upward Flow of the Fluid at Low Qualities," MIT-TR-9079-26, 1963.

16 Heineman, J. B., "An Experimental Investigation of Heat Transfer to Superheated Steam in Round and Rectangular Channels," ANL-6213, 1960.

17 Kays, W. M., *Convective Heat and Mass Transfer*, McGraw-Hill, 1966, pp. 183.

18 Nithawan, S. M., "Experimental Investigation of Thermal Non-Equilibrium in Post-Dryout Steam-Water Flow," Ph.D. Thesis, Lehigh University, 1980.

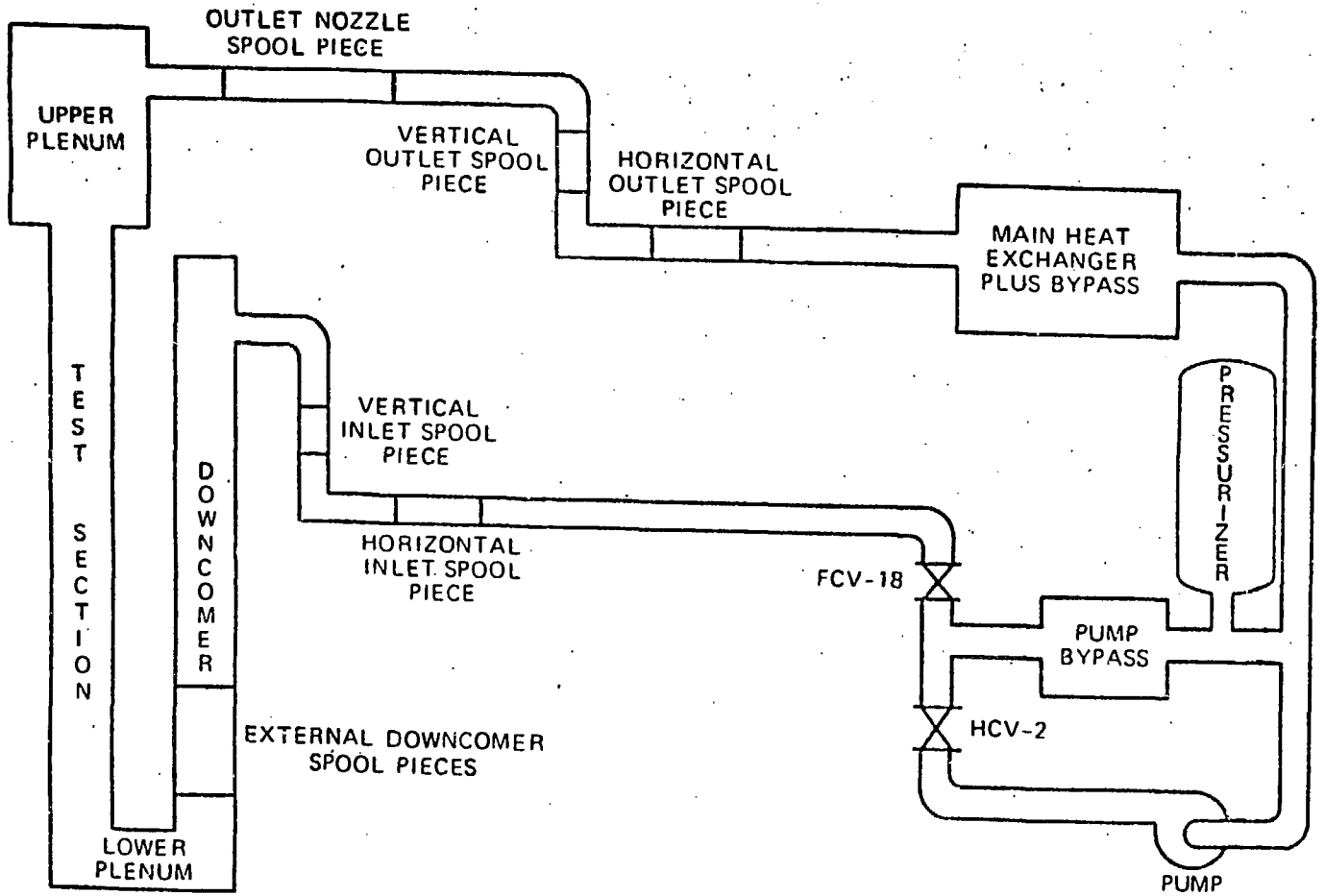


Fig. 1. Diagram of THTF.

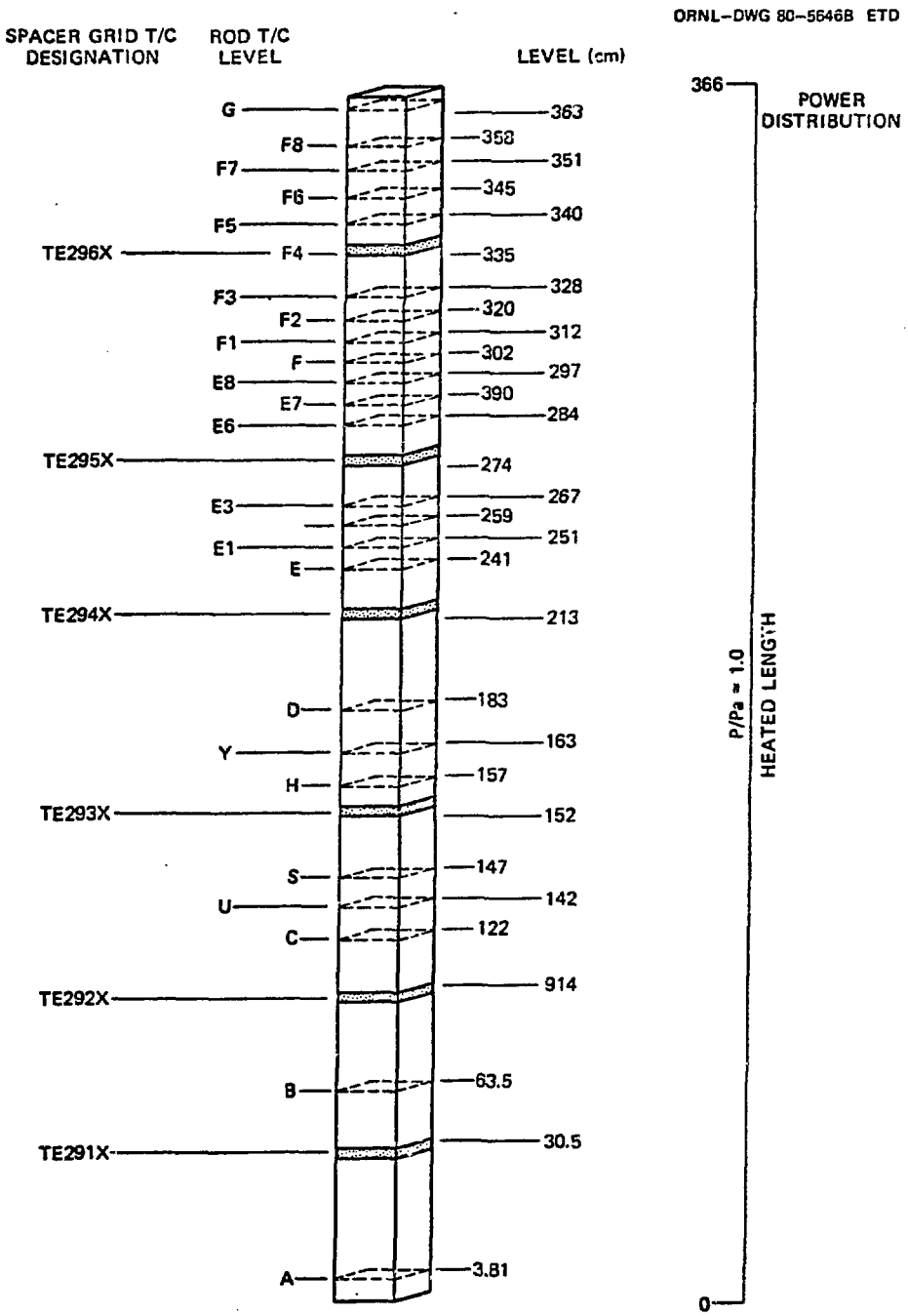


Fig. 2. Axial location of spacer grids and fuel rod simulator thermocouples.

ORNL-DWG 77-5718R

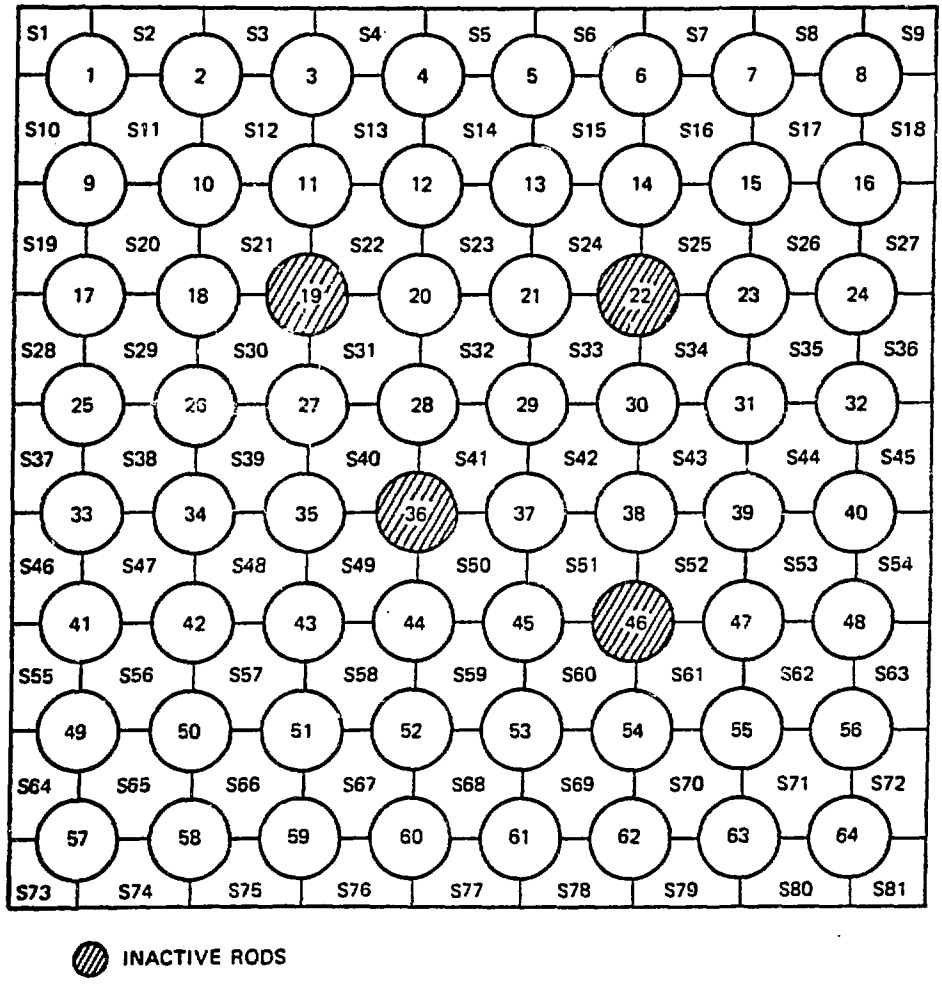


Fig. 3. Identification of THTF heater rods, subchannel locations and inactive rod in THTF heater bundle 3.

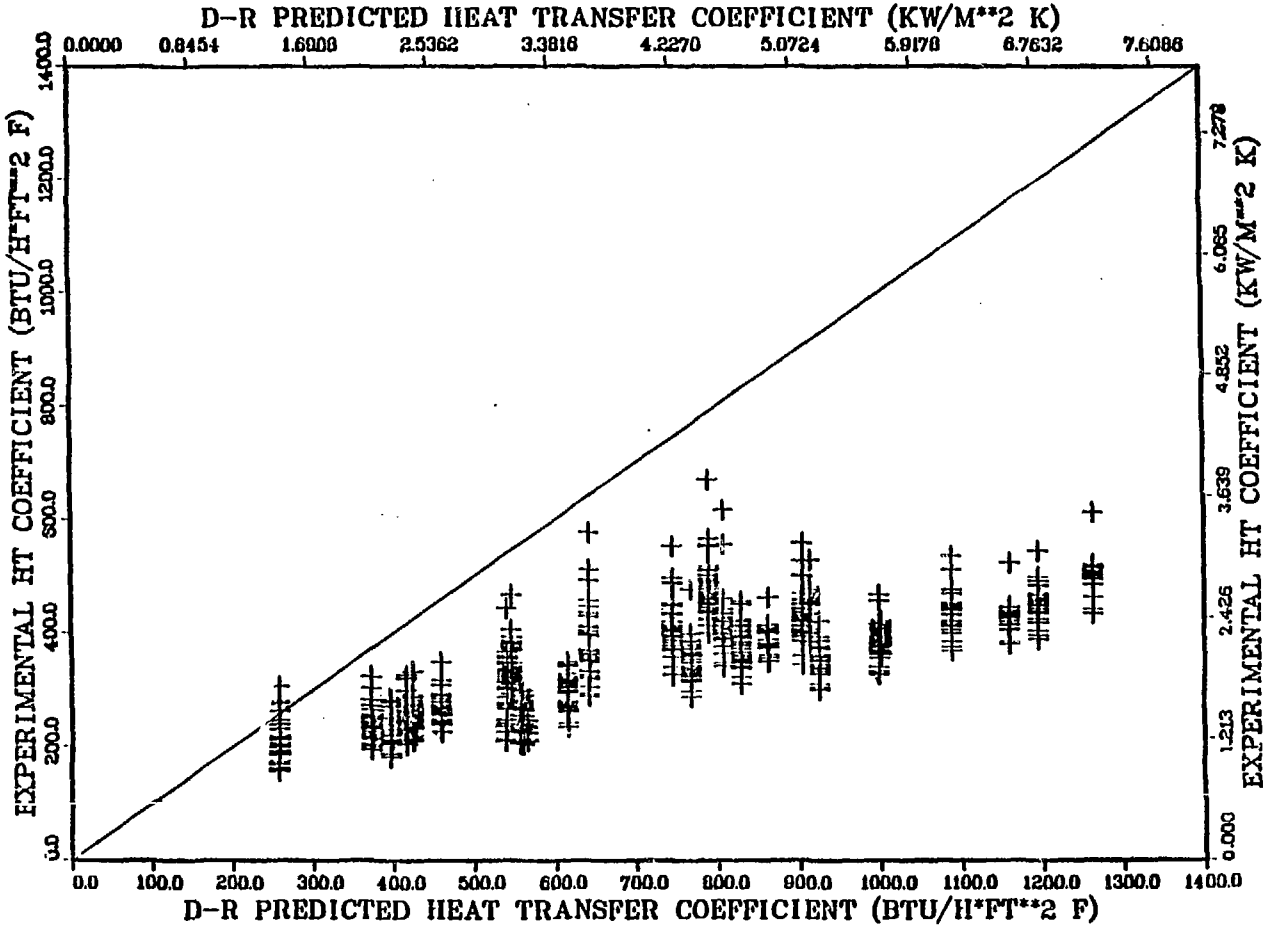


Fig. 4. $h_{exp}$ vs $h_{corr}$ for Dougall-Rohsenow, all data.

# GROENEVELD 5.7 HT CORRELATION COMPARISON

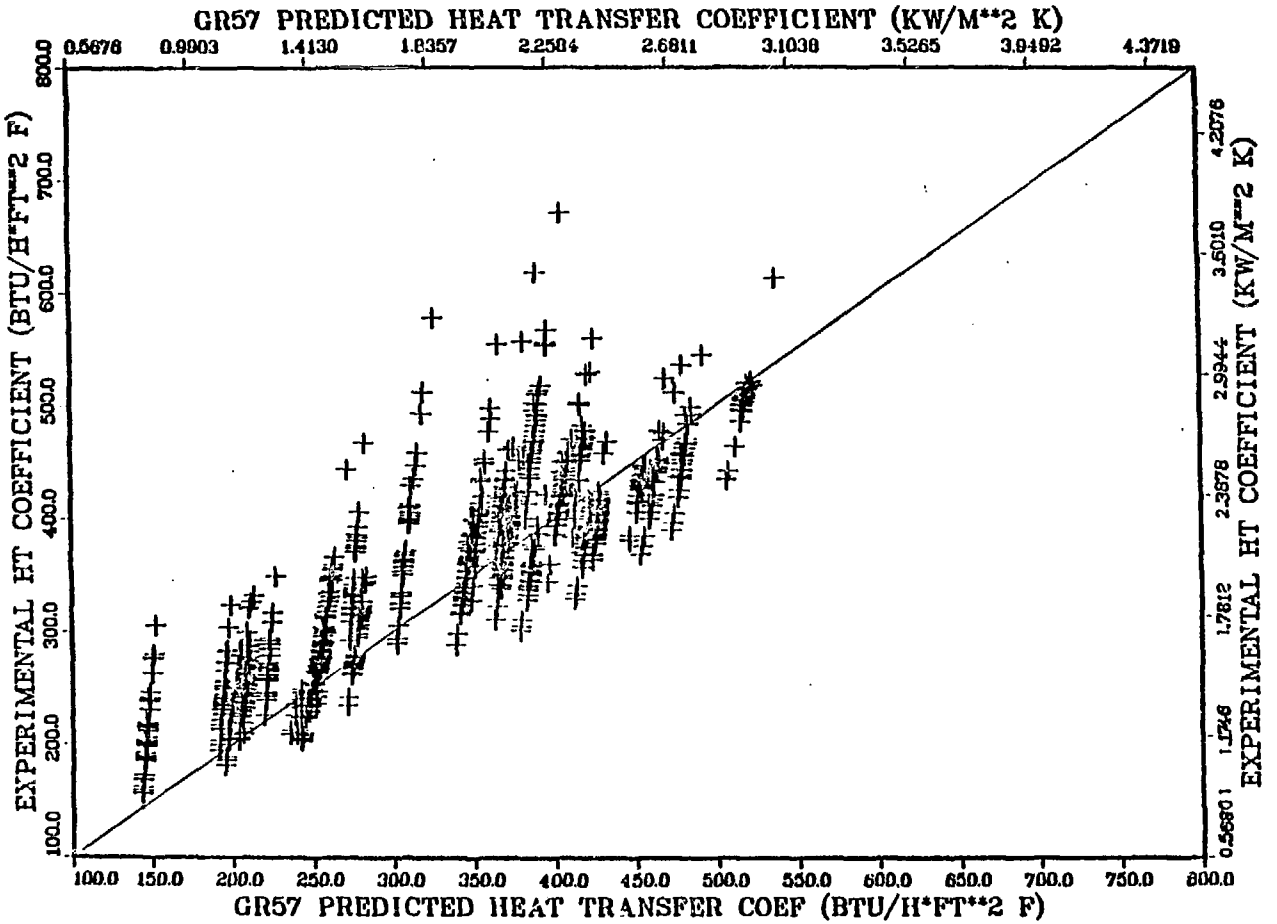


Fig. 5 $h_{exp}$ vs $h_{corr}$ for Groeneveld 5.7, all data.

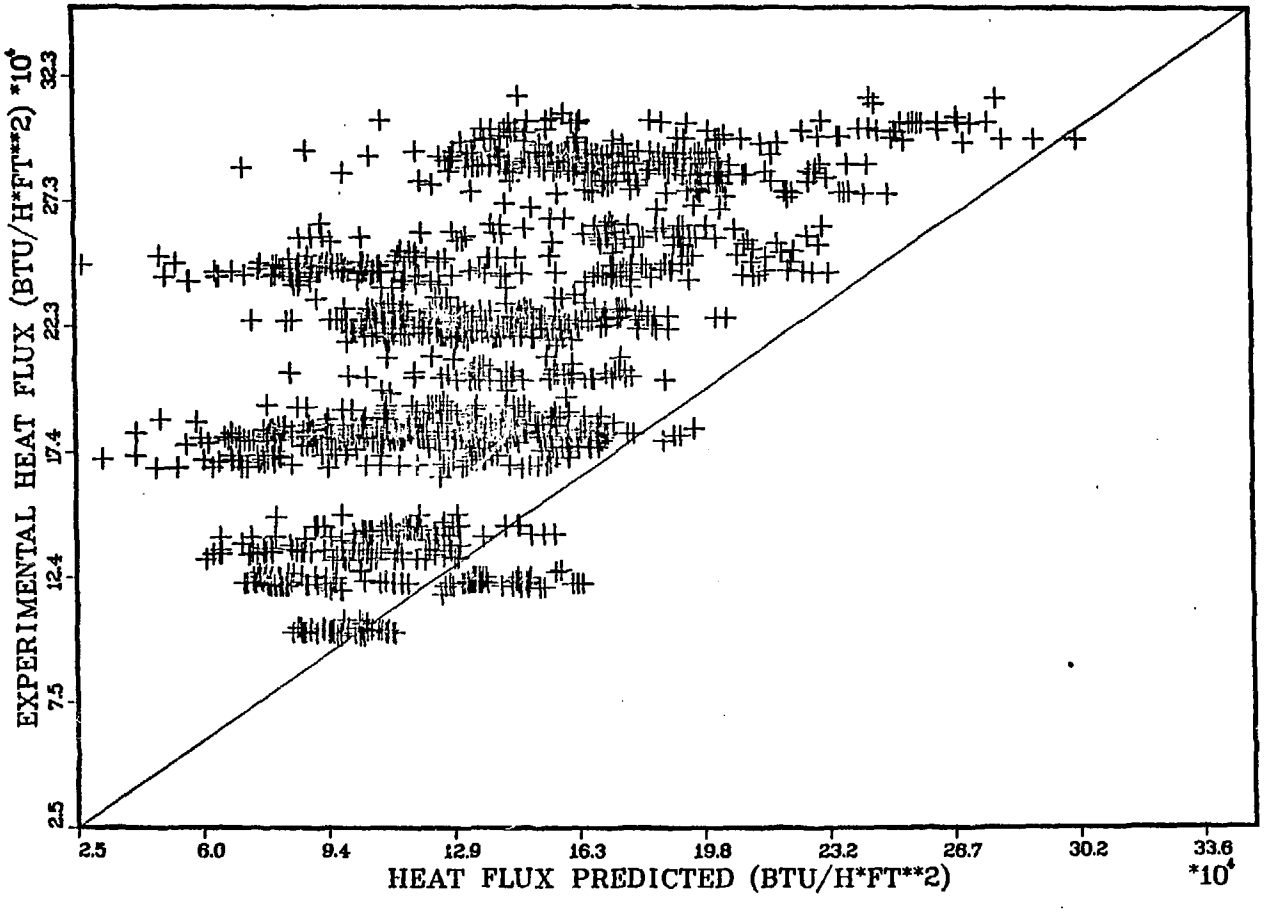


Fig. 6. $Q''_{exp}$ vs $Q''_{corr}$ for Chen nonequilibrium correlation.

# GROENEVELD SURFACE TEMPERATURE COMPARISON

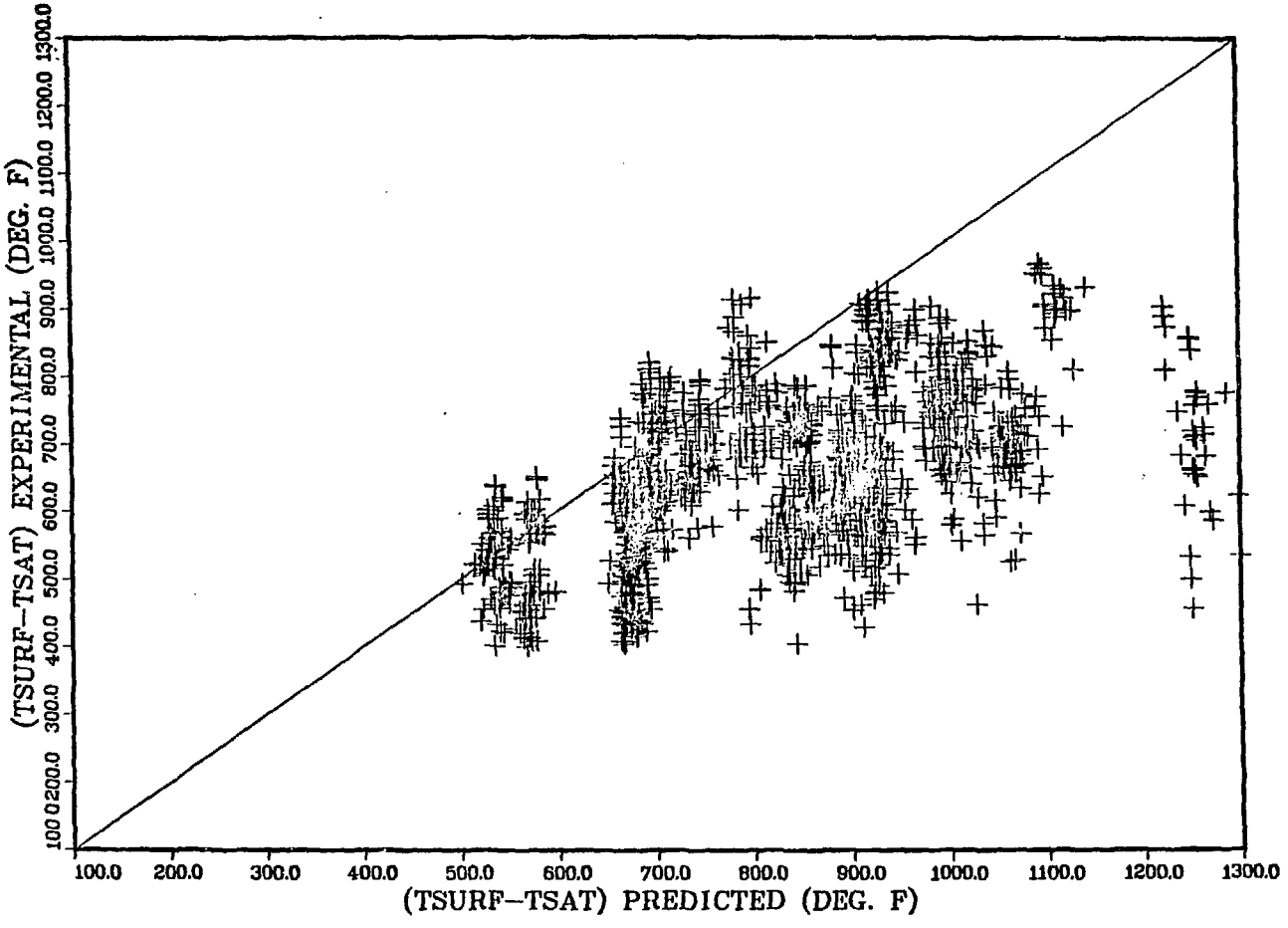


Fig. 7. Experimental wall superheat vs predicted wall superheat for Groeneveld-Delorme correlation.

# JONES SURFACE TEMPERATURE COMPARISON

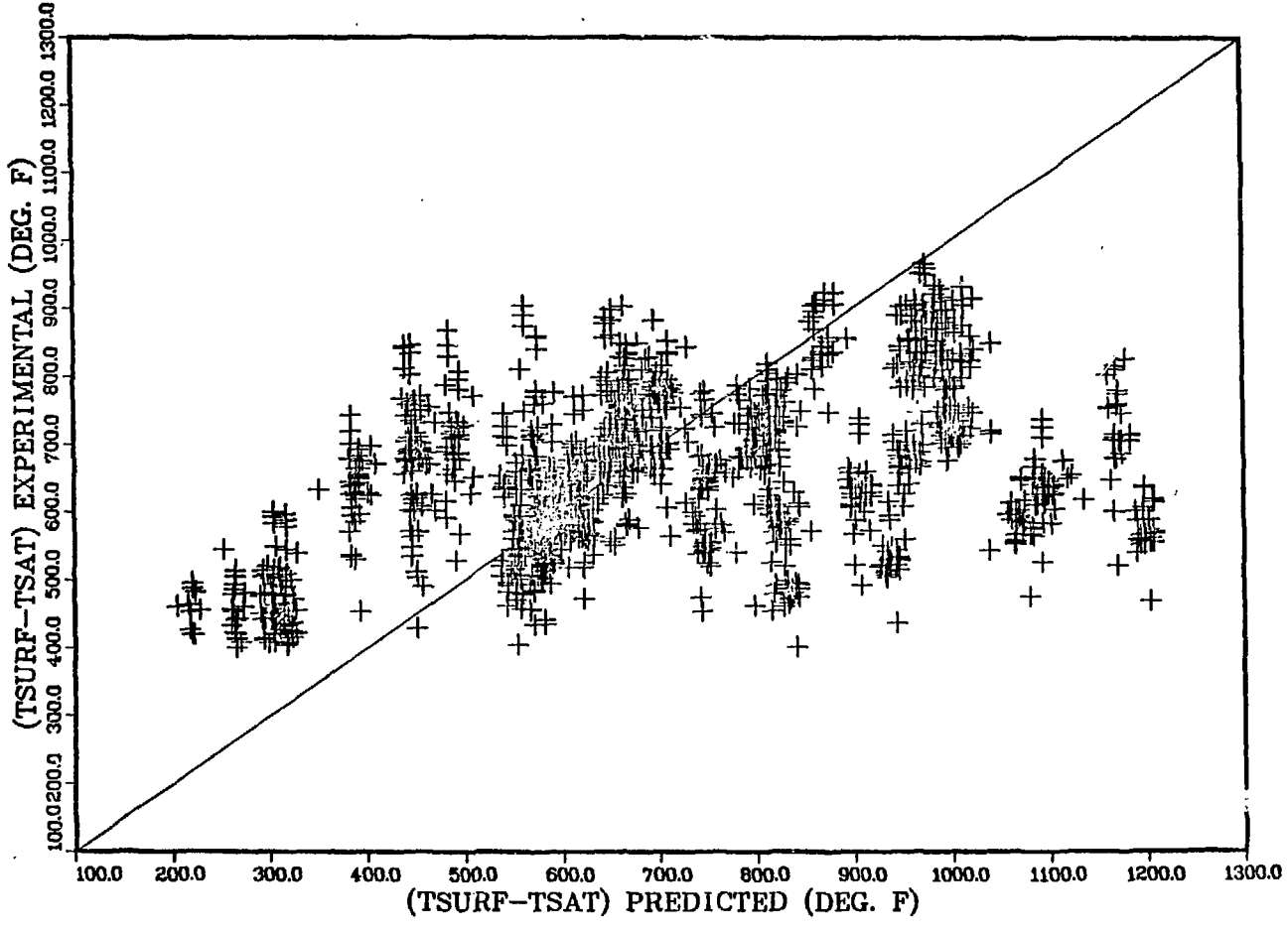


Fig. 8. Experimental wall superheat vs predicted wall superheat for Jones-Zuber correlation.

# YODER SURFACE TEMPERATURE COMPARISON

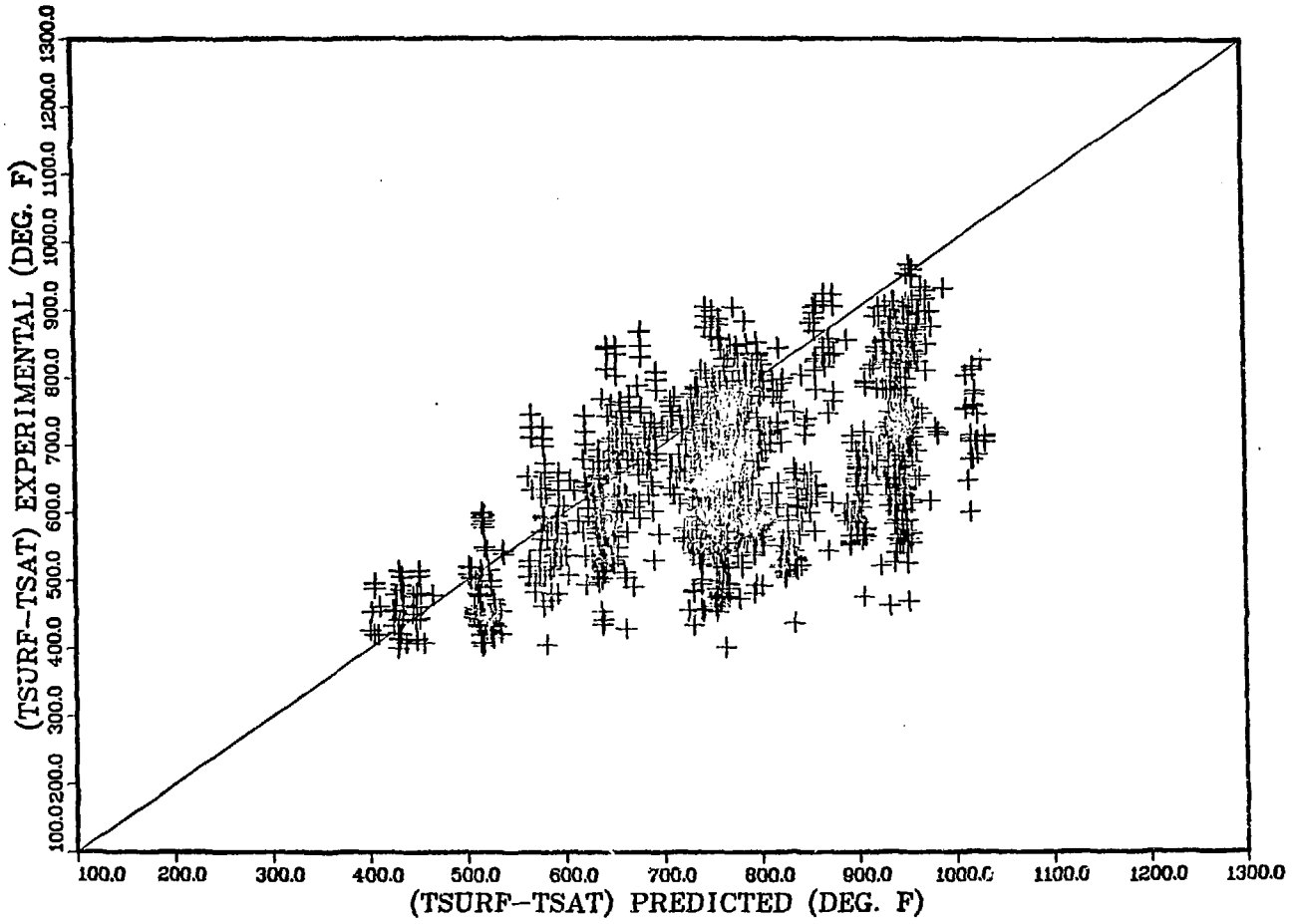


Fig. 9. Experimental wall superheat vs predicted wall superheat for Yoder-Rohsenow.